Bull. Inst. Chem. Res., Kyoto Univ., Vol.71, No.2, 1993

Observations and the Phenomenological Interpretation of Dielectric Relaxation due to Electrode Polarization

Koji ASAMI* and Tetsuya HANAI*

Received June 17, 1993

Frequency dependence of capacitance and conductance was measured of a platinum disc capacitor filled up with a 0.1M KCl aqueous solution. The observed results showed a circular arc on the complex conductance plane. Theoretical formulation is developed to represent the circular arc rule on the complex conductance plane. The electrode polarization impedance associated with the circular arc rule is also derived. The theoretical formulas derived simulate satisfactorily the observed data over the whole range of measuring frequency. Consequently the polarization impedance for the present platinum electrodes turns out to be represented phenomenologically by the simple formula.

KEY WORDS: Aqueous solution / Capacitance / Conductance / Dielectric relaxation / Electrode polarization

1. INTRODUCTION

Capacitance and conductance measurements of ionic aqueous solutions are usually carried out by using measuring cells consisting of platinum parallel plate capacitor. In this instance, the capacitance of the whole system increases and the conductance decreases with decreasing frequency.

These phenomena were observed by many workers,[1-5] having been attributed not to the specimen itself but to ionic polarization on surfaces of the platinum electrodes. As a matter of practice, dielectric measurements were usually carried out at a higher frequency side to eliminate the influence of the electrode polarization. The contribution of the electrode polarization grows dominant at lower frequencies. It is, therefore, necessary to elucidate the contribution of the electrode polarization at lower frequencies.

In the present investigation, frequency dependence of conductance and capacitance was observed over a wide range of frequency for the platinum disc electrode cells filled up with a KCl aqueous solution. The results were found to represent a circular arc on a complex conductance plane. In order to understand the characteristic dielectric relaxation, theoretical formulation was developed to represent the circular arc rule on the complex conductance plane. On the basis of the circular arc rule, a theoretical formula is also derived to express the complex conductance of the electrode surfaces. The formulas derived simulate satisfactorily the observed data over the whole range of measuring frequency. Consequently it is concluded that the complex conductance of the electrodes is represented phenomenologically by the simple formula.

* 浅見耕司, 花井哲也: Laboratory of Interface Science, Institute for Chemical Research, Kyoto University, Uji, Kyoto 611, Japan

2. THEORETICAL

2.1 Derivation of Circular Arc Formula

Hereafter, Symbols G and C denote conductance and capacitance respectively. A symbol f denotes measuring frequency in Hz unit. Subscripts l and h refer to the limit values at low and at high frequencies respectively.

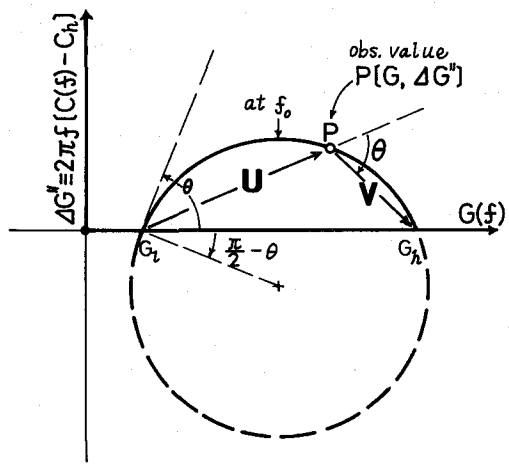

Fig.1 Complex plane plot of conductance G and imaginary part $\Delta G'' = 2\pi f \{C(f) - C_h\}$ for formulating a circular arc rule.

Figure 1 shows a complex conductance plane plots of dielectric measurements. The abscissa means real conductance $G(f)$ as a function of measuring frequency f. The ordinate denotes imaginary part $\Delta G'' \equiv 2\pi f \{C(f) - C_h\}$ at a reduction of $2\pi fC_h$ from an imaginary part $2\pi fC(f)$ of the complex conductance G^*.

A circular arc rule means that the plots of observed points $\mathbf{P}[G, 2\pi f(C - C_h)]$ at varied frequencies form part of a circle as seen in Fig.1, being formulated in the following manner.

In view of vector-sum properties on the complex conductance plane, the following relations hold for vectors $\boldsymbol{U} = \overrightarrow{G_lP}$ and $\boldsymbol{V} = \overrightarrow{PG_h}$ shown in Fig.1 .

$$G_l + \boldsymbol{U} = \boldsymbol{P} = G^* - j2\pi f C_h, \tag{1}$$

and

$$\boldsymbol{P} + \boldsymbol{V} = (G^* - j2\pi f C_h) + \boldsymbol{V} = G_h, \tag{2}$$

Here the symbol G^* indicates the complex conductance given by

$$G^* = G(f) + j2\pi f C(f), \tag{3}$$

where j is the imaginary unit defined by $j = \sqrt{-1}$.

Next, the vector $\boldsymbol{U}$ is transformed into the vector $\boldsymbol{V}$ by rotating clockwise by an angle θ and by multiplying by a factor V/U, the relationship between U and V being expressed by the following formula:

$$\boldsymbol{V} = \frac{V}{U} \times e^{j(-\theta)} \times \boldsymbol{U}, \tag{4}$$

Here the symbols U and V are the modulus of vectors $\boldsymbol{U}$ and $\boldsymbol{V}$ respectively. For simplifying the expressions, the following formulas are adopted

$$\theta \equiv \frac{\pi}{2}\beta, \tag{5}$$

and

$$e^{j\theta} = \left(e^{j\frac{\pi}{2}}\right)^{\beta} = \left(\cos\frac{\pi}{2} + j\sin\frac{\pi}{2}\right)^{\beta} = j^{\beta}, \tag{6}$$

Substitution of Eqs. (1) and (2) into Eq. (4) to eliminate $\boldsymbol{U}$ and $\boldsymbol{V}$ and the subsequent rearrangement by use of Eqs (5) and (6) give

$$G^* = G_l + (G_h - G_l)\frac{j^{\beta}\frac{U}{V}}{1 + j^{\beta}\frac{U}{V}} + j\,2\pi f C_h, \tag{7}$$

This Eq. (7) represents that an observed point $\boldsymbol{P}$ in Fig. 1 is just on the circular arc irrespective of measuring frequency.

As is shown in Fig.5 later on by experiment, plots of $\log(U/V)$ against $\log f$ shows a straight line with a slope β. This empirical linear relation is expressed as

$$\log\frac{U}{V} = \beta\log f - \beta\log f_0 = \beta\log\frac{f}{f_0}, \tag{8}$$

where f_0 means the value of f at $\log(U/V) = 0$ or $U = V$. Equation (8) is rearranged to the following form :

$$\frac{U}{V} = \left(\frac{f}{f_0}\right)^{\beta}, \tag{9}$$

Substitution of Eq. (9) into Eq. (7) gives

$$G^* = G_l + (G_h - G_l)\frac{\left(j\frac{f}{f_0}\right)^{\beta}}{1 + \left(j\frac{f}{f_0}\right)^{\beta}} + j\,2\pi f C_h, \tag{10}$$

Equation (10) is a complete formula of circular arc in the complex conductance $[G,\ 2\pi f(C - C_h)]$ plane, including a linear relationship of $\log(U/V)$ against $\log f$.

2.2 Derivation of G and C Formulas as a Function of Frequency f

Equation (10) is transformed and separated into real and imaginary parts as the followings.

$$G^* = G + j2\pi f C$$

$$= G_l + (G_h - G_l)\frac{\left(\frac{f}{f_0}\right)^{\beta}\cos\frac{\pi}{2}\beta + \left(\frac{f}{f_0}\right)^{2\beta} + j\left(\frac{f}{f_0}\right)^{\beta}\sin\frac{\pi}{2}\beta}{1 + \left(\frac{f}{f_0}\right)^{\beta}2\cos\frac{\pi}{2}\beta + \left(\frac{f}{f_0}\right)^{2\beta}} + j2\pi f C_h, \quad (11)$$

Hence we have

$$G = G_l + (G_h - G_l)\frac{\left(\cos\frac{\pi}{2}\beta + \left(\frac{f}{f_0}\right)^{\beta}\right)\left(\frac{f}{f_0}\right)^{\beta}}{1 + \left(\frac{f}{f_0}\right)^{\beta}2\cos\frac{\pi}{2}\beta + \left(\frac{f}{f_0}\right)^{2\beta}}, \quad (12)$$

and

$$C = (G_h - G_l)\frac{1}{2\pi f_0} \cdot \frac{\sin\frac{\pi}{2}\beta}{1 + \left(\frac{f}{f_0}\right)^{\beta}2\cos\frac{\pi}{2}\beta + \left(\frac{f}{f_0}\right)^{2\beta}} \cdot \frac{1}{\left(\frac{f}{f_0}\right)^{1-\beta}} + C_h, \quad (13)$$

2.3 Approximate Formulas at Low and at High Frequencies

At low and at high frequencies, Eqs. (12) and (13) are simplified as follows :

$$G(f \to 0) \simeq G_l + (G_h - G_l)\cos\frac{\pi}{2}\beta \cdot \left(\frac{f}{f_0}\right)^{\beta}, \quad (14)$$

The second term of Eq. (14) means that the straight line of log $(G - G_l)$ against log f keeps a slope β.

$$G(f \to \infty) \simeq G_h - (G_h - G_l)2\cos\frac{\pi}{2}\beta \cdot \frac{1}{\left(\frac{f}{f_0}\right)^{\beta}}, \quad (15)$$

The second term of Eq. (15) means that the straight line of log $(G_h - G)$ against log f keeps a negative slope $-\beta$.

$$C(f \to 0) \simeq C_h + (G_h - G_l)\frac{1}{2\pi f_0}\sin\frac{\pi}{2}\beta \cdot \frac{1}{\left(\frac{f}{f_0}\right)^{1-\beta}} \quad (16)$$

The second term of Eq. (16) means that the straight line of log $(C - C_h)$ against log f keeps a negative slope $-(1-\beta)$.

$$C(f\to\infty)\simeq C_h+(G_h-G_l)\frac{1}{2\pi f_0}\sin\frac{\pi}{2}\beta\cdot\frac{1}{\left(\frac{f}{f_0}\right)^{1+\beta}} \tag{17}$$

The second term of Eq. (17) means that the straight line of log $(C-C_h)$ against log f keeps a negative slope $-(1+\beta)$.

Some examples of numerical calculation for Eqs. (12) and (13) are shown in Fig.2. In the figure, the capacitance C increases and the conductance G decreases with decreasing frequency over a frequency range lower than 100 kHz. At frequencies lower than 100 Hz, the increasing tendency of C with decreasing frequency is reduced as compared with that in the higher side of frequency. It is seen in Fig.2 that the capacitance C increases infinitely at still lower frequencies except for $\beta=1$.

Johnson and Cole[3] have already presented formulas of the frequency dependence of C and G concerning the electrode polarization. Their formulas are in full accord with Eqs. (15) and (17). They presented no formulas corresponding to Eqs. (14) and (16) for lower frequencies.

2.4 Derivation of Complex Conductance G_p^* for Electrode Polarization

Hereafter, subscripts p and w refer to the electrode polarization and the aqueous specimen respectively.

It is natural to assume that the whole complex conductance G^* is a series combination of a complex conductance G_p^* for the electrode polarization and a complex conductance G_w^* for the aqueous specimen. Hence the G_p^* is expressed as

$$G_p^*=\frac{G_w^*G^*}{G_w^*-G^*}, \tag{18}$$

In the present set of experiments, the following relationship holds for a series combination of platinum electrodes and the aqueous specimens.

$$G_l(\sim 0.001\text{mS})\ll G_h(\sim 5\text{mS})\fallingdotseq G_w, \tag{19}$$

$$C_h(\sim 8\text{pF})\fallingdotseq C_w\ll G_w/(2\pi f_0)\equiv C_0(\sim 1\,\mu\text{F}), \tag{20}$$

where C_0 is defined by this Eq. (20). By use of Relations (19) and (20), Eq. (10) is reduced to

$$G^*\simeq\frac{G_w\left(j\frac{f}{f_0}\right)^{\beta}}{1+\left(j\frac{f}{f_0}\right)^{\beta}} \tag{21}$$

Substitution of Eq. (21) into Eq. (18), and the subsequent rearrangement lead to a simple formula for G_p^* as follows :

$$G_p^*\simeq G_w\left(j\frac{f}{f_0}\right)^{\beta}\simeq G^*\left(j\frac{f}{f_0}\right)^{\beta} \tag{22}$$

Equation (22) shows that the electrode impedance G_p^* is a simple function form characterized by β, f_0 and G_w.

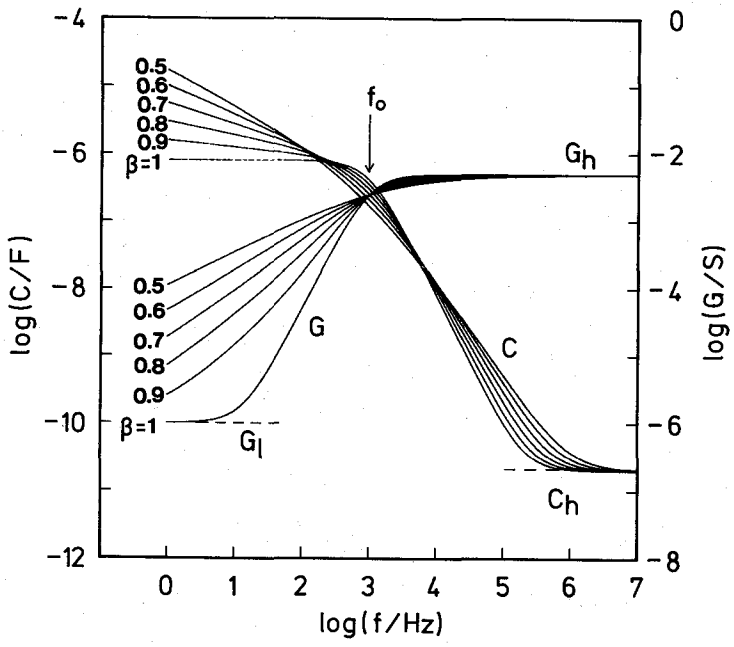

Fig.2 Frequency dependence of capacitance C and conductance G calculated from the theoretical formulas Eqs. (12) and (13) expressing the circular arc on a complex conductance $[G, \Delta G^*]$ plane.
Parameter values adopted: C_w=20 pF, G_w = 4.999 mS, G_l= 0.001 mS, f_0 = 1 kHz, β = 1, 0.9, 0.8, 0.7, 0.6 and 0.5 .

3. EXPERIMENTAL

The measuring cell, made of methyl methacrylate resin, consisted of a pair of platinum disc electrodes. The effective diameter of the disc electrodes was 5mm, the distance between the two electrodes being 5.5mm. Two kinds of electrodes were investigated: the one is platinum electrodes (without platinum black), the other being platinized platinum electrodes (coated with platinum black). The Pt electrode cells were filled up with a 0.1M KCl aqueous solution for the measurements.

Dielectric measurements were carried out with a YHP 4192A LF-Impedance Analyser operating in a frequency range from 5Hz to 13MHz. All the measurements were carried out at 25℃.

4. RESULTS AND DISCUSSION

Figure 3 shows observed results on frequency dependence of conductance G and capacitance C for the cells consisting of platinum electrodes and of platinized platinum electrodes, both being filled with a 0.1M KCl solution. Remarkable increase in C and decrease in G are found at frequencies lower than 100kHz. The increasing tendency of C with decreasing frequency is reduced at still lower frequencies below 100Hz, suggesting absence of any upper limits at still lower frequencies. The dielectric relaxation of C and G shown in Fig.3 is supposed to be attributed to electrode polarization.

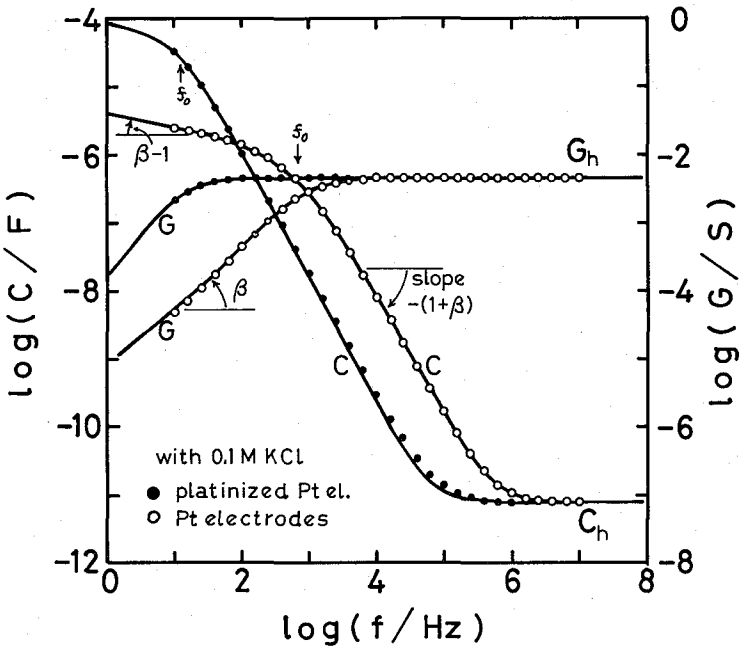

Fig.3 Frequency dependence of capacitance C and conductance G observed on a Pt electrode-KCl solution system. Filled circles ● are the observed data for a platinized Pt electrode cell filled up with a 0.1 M KCl solution, hollow circles ○ being for a Pt electrode (no Pt-black) system. The solid curves are calculated from theoretical Eqs. (12) and (13) using parameter values shown in Table 1.

The same data are plotted on a G- $\Delta G''$ plane in Fig.4. Evidently the plots of data shown in Fig.4 represent circular arcs characterized by G_h, G_l and θ. The same data are plotted on a $\log(U/V)$ - $\log f$ plane in Fig.5, yielding a straight line with a slope β and an abscissa intercept f_0 at $U/V = 1$.

These results realize the characteristics of a circular arc (Fig.4) and of the linear relation between $\log(U/V)$ and $\log f$ (Fig.5). The formulation developed in the preceding Theoretical Section, therefore, is effective for simplifying and summarizing the data observed.

Values of β and f_0 are obtained from the plots of data in Fig.5, being listed in Table 1

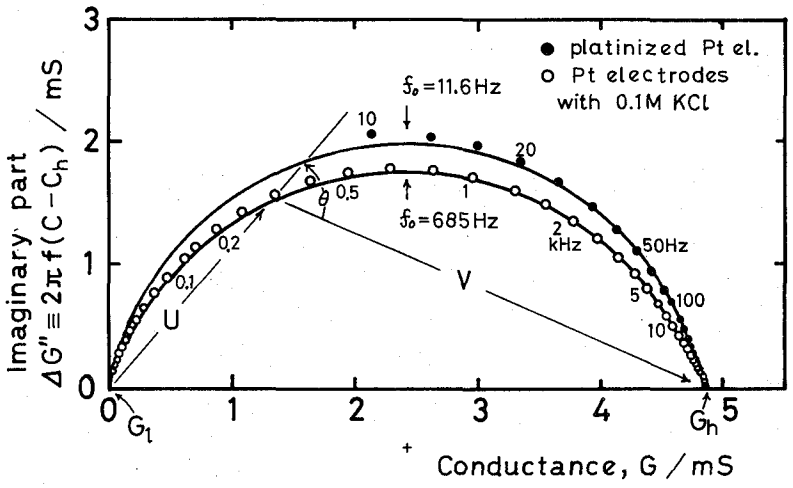

Fig.4 Complex plane plots of complex conductance $[G, \Delta G'']$ for the Pt electrode-KCl solution systems. The same data as shown in Fig.3. Filled circles ● are the observed data for a platinized Pt electrode cell filled up with a 0.1 M KCl solution, hollow circles ○ being for a Pt electrode (no Pt-black) system. The solid curves are calculated from Eqs. (12) and (13) using parameter values shown in Table 1.

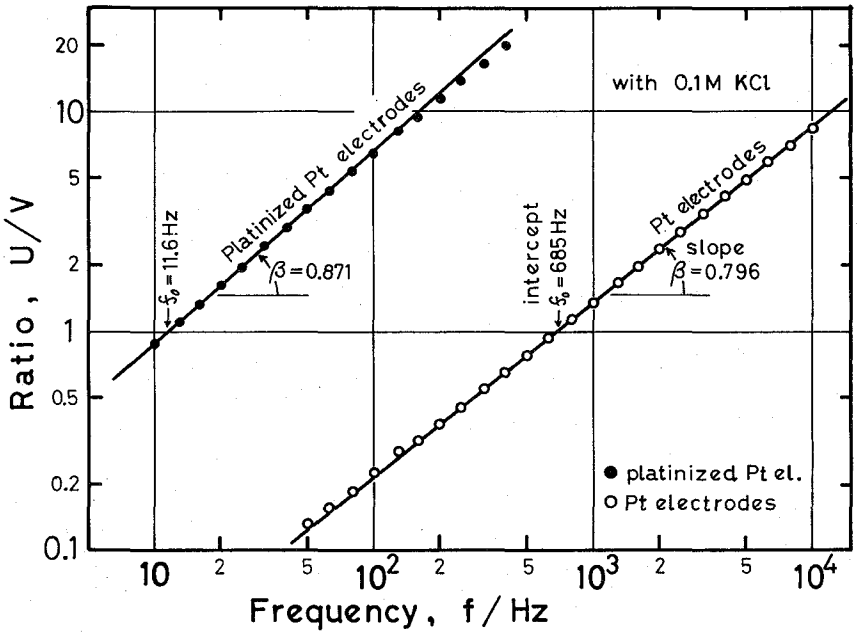

Fig.5 Plots of $\log(U/V)$ against $\log f$ for the data shown in Figs.3 and 4. Filled circles ● are the observed data for a platinized Pt electrode cell filled up with a 0.1 M KCl solution, hollow circles ○ being for a Pt electrode (no Pt-black) system.

Table 1. Values of parameters β, f_0, G_h and C_h characterizing the circular arc on the $[G,\ \Delta G'' \equiv 2\pi f(C - C_h)]$-plane. The cells are filled up with a 0.1M KCl aqueous solution.

Electrode	β	f_0/Hz	G_h/mS	C_h/pF
Platinum Electrode (no Pt - black)	0.796	685	4.83	8.07
Platinized platinum electrode	0.871	11.6	4.85	8.00

together with the values of G_h and C_h obtained from Fig.3.

By use of the values listed in Table 1, theoretical curves following the circular arc rule are calculated from Eqs. (12) and (13), being shown by solid curves in Figs.3 and 4. The theoretical curves simulate satisfactorily the observed data over the whole range of measuring frequency.

It is, therefore, concluded that the electrode polarization of platinum electrodes are represented phenomenologically by Eq. (22). The detailed electrochemical mechanism of the electrode impedance represented by Eq. (22) must await further exploration.

REFERENCES

(1) H. Fricke, *Phil. Mag.*, **14**, 310 (1933).
(2) J. D.Ferry, J. L. Oncley, *J. Amer. Chem. Soc.*, **63**, 272 (1941).
(3) J. F. Johnson, R. H. Cole, *J. Amer. Chem. Soc.*, **73**, 4536 (1951).
(4) W. Dannhauser, R. H. Cole, *J. Amer. Chem. Soc.*, **74**, 6105 (1952).
(5) T. Hanai, N. Koizumi, R. Gotoh, *Kolloid Z.*, **167**, 41 (1959).